Supercapacitor modified with Methylene Blue as redox active electrolyte

*Silvia Roldán, Marcos Granda, Rosa Menéndez, Ricardo Santamaría and Clara Blanco**

Instituto Nacional del Carbón, CSIC, Aptdo. 73, 33080-Oviedo, Spain

clara@incar.csic.es

ABSTRACT.

MWCNT-based supercapactors (SC) containing methylene blue (MB) as redox active electrolyte were studied. MWCNTs were employed as model of electrode active material due to their ideal double-layer behavior facilitates the investigation of the energy storage mechanisms involved. MB led to a cell capacitance enhancement equal to 4.5 times the original cell capacitance of MWCNTs in sulphuric acid with a capacitance reduction of only 12 % after 6000 charge-discharge cycles. The potential evolution of each electrode during galvanostatic cycling revealed that MB redox reaction develops in both electrodes simultaneously in the voltage range of 0-0.104 V and that this is the main cause of cell capacitance enhancement. Beyond this voltage range, the faradaic contribution from the MB redox reaction decreases because the anode behaves as a capacitative electrode with a rather reduced charge-capacity due to the small surface area of MWCNTs. By means of a modified assembly composed of a Nafion membrane and MB and sulfuric acid solutions located in the cathode and anode compartments, respectively, it was demonstrated the limiting role of the capacitative electrode in the cell charge-capacity in this type of hybrid devices.

*Corresponding author. Tel.:+34 9 85119090; Fax: (+34) 985 297 662

E-mail address: clara@incar.csic.es

KEYWORDS. Methylene blue, multiwalled carbon nanotubes, faradaic reactions, redox electrolyte, supercapacitor.

1.- INTRODUCTION

Supercapacitors (SCs) are energy storage devices that have attracted great attention because they can store higher energy than dielectric capacitors and, simultaneously, deliver higher power in a shorter time than batteries. SCs based on carbon materials (CBSCs) have been the most developed and employed in commercial applications to date due to their excellent properties, such as low cost, good electronic conductivity, large capacitance and long cycling life[1,2]. Thanks to these characteristics, CBSCs are used in a great number of electronic devices. However, for their use in certain potential applications, such as hybrid electric vehicles, it is first necessary to increase their energy density[3]. In this context, a great deal of effort has been made in order to increase the energy stored by CBSCs, these being for the most part centred on capacitance enhancement through the use of pseucapacitive contributions provided by functional groups from physical /chemical activations[4,5], oxidation with strong acid, bases or air[6], or polymers deposition[7,8]. However, as it is well known, the enhancement of capacitance by pseudocapacitive contributions is significantly sensitive to long-term cycling because functional groups generated during the above treatments are usually unstable and disappear with cycling[5,9,10] or, in the case of conducting polymers, suffer shrinkage and swelling which lead to the gradual degradation of the electrodes[8,11,12].

Our research group has recently proposed a highly efficient and low cost alternative route to enhance cell capacitance, based on the incorporation of an electrochemically active molecule (such as hydroquinone or indigo carmine) into the SC electrolyte[11-15]. Capacitance increases up to 4.5 times the original capacitance value with no significant modification of the equivalent series resistance (ESR) of the device can be achieved with this simple method, which have led to a carbon-based device[12] with a maximum energy density of 31 Wh Kg^{-1},[14] close to that of some batteries[16].

The main aim of this work is to provide further insight into the energy storage mechanisms involved in devices based on active redox electrolytes, analyzing in detail the role played by both electrodes when the Faradaic reaction of the redox molecule develops in the negative electrode. The redox system selected for this purpose was Methylene blue (MB), an organic dye with outer-sphere electron transfer reaction[17], able to promote a great capacitance enhancement with an exceptional durability related. The study was developed using MWCNTs as model of electrode active material due to the fact that their ideal double-layer behaviour simplifies the theoretical discussion concerning energy storage mechanisms. This work complements our previous study on a hybrid device with a battery-type positive electrode[15], offering in conjunction a broad analysis of the capacitance enhancement in this type of systems.

2.- EXPERIMENTAL

2.1. Electrolytes

All of the solutions were prepared using analytical grade reagents and used immediately after their preparation. A 0.07 M solution of methylene blue (MB), 3,9-bis(dimethylamino)phenazothionium chloride, dissolved in 1 M H_2SO_4 (MB-H_2SO_4) was employed as redox-active electrolyte. Methylene blue with a purity > 95% was supplied by Sigma-Aldrich. The supporting electrolyte, a 1 M solution of H_2SO_4 supplied by Prolabo, was also studied for comparative purposes.

2.2. Electrode material

Multiwalled carbon nanotubes (MWCNTs), supplied by Sigma-Aldrich, were used as active electrode material. The apparent specific surface area of the carbon sample, determined by physical

adsorption of N_2 at 77 K in an *ASAP 2020 Micromeritics* volumetric system using the BET equation, was equal to 210 m^2 g^{-1} and the average pore size was 2 nm.

2.3. Electrode preparation and electrochemical characterization

The electrodes were prepared in the form of pressed pellets of diameter 12 mm using a mixture of MWCNTs (90 wt%) and Teflón® (10 wt%) as binder. Two electrode capacitors were built in Swagelok® systems using gold discs as current collectors and glassy fiber separators.

The capacitors were electrochemically characterized by cyclic voltammetry (at 2mV s^{-1}) and cyclic chronopotentiometric experiments (from 0.9 to 88.4 mA cm^{-2}) performed using a VMP (Biologic) multichannel generator in an operating voltage window of 1 V. The capacitance of each device was expressed as cell capacitance, which was deduced from the discharge curve avoiding the ohmic drop: $C_{cell} = I\ (dt/dV)$, where I is the current intensity and dV/dt is the slope of the discharge curve. The cell capacitance values were divided by the total mass of active material in both electrodes in order to express them as a specific capacitance.

The electrochemical reactions of MB were characterized by cyclic voltammetry using a three-electrode system obtained by incorporating the Hg/Hg_2SO_4 electrode as reference into a T-type Swagelok® cell. The MWCNTs were used as active electrode material in both the working and auxiliary electrode. The intensity measured was referred to the total active material of the cell in order to facilitate comparison between the different devices.

The same configuration was employed to study the potential evolution of each electrode during the galvanostatic cycling (at 8.84 mA cm^{-2}) of the device. This system was then modified using a Nafion membrane as separator in order to study the role of the positive electrode in the faradaic process of MB. The capacitance of each electrode in each system was calculated from the quantitative treatment previously published[15].

All the electrochemical experiments were carried out at ambient temperature.

3.- RESULTS AND DISCUSSION

Fig. 1a shows the variation of cell specific capacitance values at increasing current densities for the original double-layer capacitor and for the device modified with MB. As can be clearly seen, the incorporation of MB is a very advantageous modification for enhancing cell capacitance, as it increases the original cell capacitance by 4.5 times (from 5 to 22.6 F g^{-1}; from 21 to 96 F g^{-1} per mass of electrode). Furthermore, this enhanced performance is maintained over almost the whole range of current densities tested with no significant change in the ESR (0.5 Ω cm^2 for the EDLC and 0.75 Ω cm^2 for MB-based device) and with only a 10% loss of capacitance with current load.

The long-term cycling performance of the modified device was also studied since durability is considered one of the most important requirements for assessing the suitability of an energy storage device for practical applications[18]. Capacitance values proved to be highly stable during cycling, with a reduction of only 12 % after 6000 charge-discharge galvanostatic cycles recorded at a current regime of 8.84 mA cm^{-2}. The efficiency and ESR values also proved to be stable throughout the cycling test, with values of around 98 % and 0.8 Ω cm^2, respectively. The small loss of capacitance during the cycling is essentially due to the characteristics of the MB redox reaction responsible for the capacitance enhancement in this system which, as it will be seen below, corresponds to a highly reversible electrochemical process within the working potential range of the device.

It is hence noteworthy the great potential of MB for enhancing the performance of a nanotube-based capacitor, as it leads to capacitance increases comparable or even greater than those achieved by treatments such as oxidation with strong acids or bases or by the incorporation of conducting polymers. At the same time, treatment with MB gives rise to a device highly stable with the current density and

much greater efficiency for long durability than devices dependent on pseudocapacitive contributions that are typically unstable with cycling[5,8,9].

As might be expected, the electrochemical reaction of MB greatly modifies the shape of both the chronopotenciometric and voltammetric cycles (Fig. 1b, 1c), from the typical profiles of a pure electrostatic interaction consisting of triangular galvanostatic cycles and almost rectangular voltammograms, to the appearance of plateaus of potential (Fig. 1b) and well-defined redox peaks (Fig. 1c) characteristic of the combination of an electrostatic charge storage mechanism with one of a Faradaic kind[19]. Nevertheless, the most reliable technique for analyzing the electrochemical characteristics of any Faradaic process is cyclic voltammetry developed in a three-electrode configuration. Figure 2a shows cyclic voltammograms recorded at 2 mV s^{-1} in a three-electrode configuration for both electrolytes. The main peak (labeled A) in the voltammetric profile of the modified device, with a midpoint potential ($E_{1/2}$) of -0.208 V (vs. Hg/Hg_2SO_4), is characterized by a stable and well-defined electrodic signal with oxidation and reduction peaks of the same intensity located at E_a= -0.188 V and E_c= -0.227 V, respectively, and a peak potential difference (ΔE_p) of 34 mV. These potential values are very close to those found in the literature for the MB redox reaction in similar conditions[20,21]. In addition, the ΔE_p value approaches the expected theorical value for a two-electron reversible process, indicating that this reaction involves a fast electron transfer. According to these considerations, these peaks should be attributed to the two-electron process of MB in acidic media[20,22,23] illustrated in Scheme 1.

In order to elucidate the current control process, the scan rate was varied from 1 to 50 mV s^{-1} and a linear relationship between the square root of the scan rate on the anodic and cathodic peak current was found (Fig. 2 b), which demonstrates that the electrochemical response of MB is diffusion-controlled under these experimental conditions. This result is in agreement with the strong tendency of adsorption of this dye, which explains why the reaction mechanism must be controlled by the transport of ions to and from or through the electrode interface[24,25].

The more negative peaks with $E_{1/2}$= 0.278 V (labeled B) can be ascribed to the same MB reaction, being its lower intensity signal due to changes in the capacity of charge compensation of the auxiliary electrode within this range of potentials, which will be explained in detail below.

Finally, it should be mentioned that during cycling, the partial dissolution of the Fe catalyst residual nanoparticles of CNTs and their subsequent redox reaction give rise to the reversible electrodic signal located at $E_{1/2}$= 0.022 V (labeled C), which appears in both the voltammograms recorded in MB and in the sulfuric acid solution with the same intensity. The presence of metal catalyst particles in purified carbon nanotube materials has been extensively reported in the literature[26-28]. These metallic particles are predominantly located at the base of the nanotubes, on its tip or encased inside them and entrapped within the graphene layers or covered by thin layers of amorphous carbon. They may exhibit electrocatalytic effects[29] and redox activity or even dissolve and show electrochemical activity in solution[30] depending on the supporting electrolyte composition, as was demonstrated by J. L. Lyon el at[31]. The electrodic process observed occurs at the potential expected for the Fe^{3+}/Fe^{2+} reaction in sulfuric acid[32]. Therefore, it can be stated that iron from the nanotubes increases the capacitance provided by the electric double layer though a faradaic reaction that develops in the same extent in the original EDLC and in the device modified with MB.

It is also worth noting that after the incorporation of MB the baseline current remains the same as in the supporting electrolyte over the whole range of potentials employed, making it easy to identify the potential interval in which the Faradaic contribution from the MB redox reaction occurs (from -0.350 V to -0.130 V vs. Hg/Hg_2SO_4).

To obtain further insight into the role played by the MB in the energy storage process, the behaviour of both electrodes was analyzed in detail by recording their potential evolution during galvanostatic cycling at 8.84 mA cm^{-2}, before and after the incorporation of the redox molecule (Fig. 3a, b). In addition, both the capacitance of each electrode and the cell capacitance were calculated in order to analyze each system quantitatively (Table 1). As might be expected for an EDLC, the cell

voltage is evenly divided between the electrodes in the original capacitor (Figure 3a), the capacitance of each one being exactly the same and equal to double the cell capacitance (Table 1, capacitance expressed in Farads).

However, as it can be seen from Figure 3b, when MB is incorporated into the electrolyte both the working potential range of the electrodes and the equilibrium potential of the system (which depends on the electrode material and the electrolytic media) are modified, this being the key factor to explain the overall working of the modified device. The rest potential shifts from 0 V in the original capacitor to -0.2 V vs. Hg/Hg_2SO_4 in the MB-modified device. Thus, when the cell is completely discharged (0 V for the two-electrode cell) both electrodes are at the potential of the MB redox reaction, which is the value that separates the anode and cathode working potential intervals: from 0.482 to -0.200 V vs. Hg/Hg_2SO_4 for the anode and from -0.200 to -0.529 V vs. Hg/Hg_2SO_4 for the cathode. In the light of these considerations and given the location of the MB main redox peak (labeled A) on the three-electrode voltammogram (Fig. 2a), it can be assumed that both electrodes take part in the MB electrochemical process.

Thus, during the charging process both electrodes exhibit simultaneously a battery-type behaviour within the voltage range of 0-0.104 V (region I in Fig. 3b), characterized by an almost total lack of variation in potential with time due to the fact that the main energy storage mechanism is of Faradaic kind in which the voltage (V) is practically independent of the charge (q)[19,33]. In this operating voltage the potential interval of the cathode and anode (Table 2) delimits exactly the main redox peak of MB (peak A) recorded in Fig. 2a. It is important to point out that in this region the overall system behaves like a battery in which the same redox species is present in both electrodes and, therefore, the performance of the system as battery will be limited by the electrode in which the reaction develops in a lesser extension. As can be seen in Fig. 3b, the limiting electrode is the anode, since the cathode continues to exhibit a battery-type behaviour until it reaches a potential value of -0.35 V vs. Hg/Hg_2SO_4.

In the working voltage range corresponding to region II (Table 2), the MB redox reaction developed in the cathode gives rise to a second peak (labeled B) of lower intensity in the three-electrode voltammogram (Fig. 2a). This reduction in peak intensity is caused by the lower capacity of charge compensation provided by the anode in this voltage region, where this electrode operates between -0.142 and 0.432 V vs. Hg/Hg_2SO_4. According to the three-electrode voltammogram, charges from the Faradaic reaction of MB are compensated in the anode by two energy storage processes: the electrochemical reaction of Fe catalyst nanoparticles, which appears as a plateau between -0.053 and 0.099 V vs. Hg/Hg_2SO_4 in Fig. 3b, and the charging of the electric double layer. Due to the differences between the energy storage processes in both electrodes, the device behaves as a hybrid system in this voltage range and, therefore, it is possible to consider that the double-layer full charge capacity of the anode is employed to compensate the charges from the cathode due to the latter's battery-type behaviour[19].

Finally, the system behaves as an EDLC in the voltage range III (Table 1, Fig. 3b), where both electrodes display a mainly capacitor-type behavior characterized by a variation of the electrode potentials determined by the relationship existing between capacitance, charge and voltage (C=q/V).

From a quantitative point of view (Table 2), the incorporation of MB significantly increases the capacitance of both electrodes, although not to the same extent due to the different degree to which the redox reaction of this molecule develops in each electrode. While the anode increases its capacitance 3.4 times after the addition of the redox molecule, the cathode multiplies its original capacitance by 6.6 due to its behaviour as a battery over almost the overall voltage range. As a consequence of the increase in capacitance in both electrodes, the net overall capacitance is also greatly enhanced, from 5 to 23 $F\ g^{-1}$, being the value reached obviously limited by the smaller of the two electrode capacitances because of the relationship that exists between the capacitance of each individual electrode and cell capacitance, i.e., $1/C_{cell} = (1/C_{cathode}) + (1/C_{anode})$.

According to the above discussion, it can be said that the capacity of MB to enhance the capacitance of the device is directly related to the battery-type behaviour of the cathode and the capacity of the anode to compensate charges from the redox reaction. To clarify this concept, the response of the system was studied in a T-type cell modified with a Nafion membrane as separator, which allows protons to pass through it but prevents the passage of MB molecules, the cathode and the anode compartments containing solutions of MB and sulfuric acid, respectively. The absence of MB in the anode leads to the disappearance of the battery-type behaviour of the positive electrode (Fig. 3c) and, therefore, of the overall system. In this situation charges from the MB Faradiac reaction are compensated in the positive electrode only by the charging of the electric double layer and the Fe nanoparticle redox reaction. As a consequence, the capacitance of the anode is reduced until almost its value in the original EDLC (Table 1), while the cathode exhibits a battery-type behaviour over the overall voltage range because of the inability of the positive electrode to compensate all the charges from redox reaction. Under these conditions, the capacitance of the faradaic electrode can be considered infinite with respect to the capacitance attained by the capacitative electrode. Thus, cell capacitance is determined by anode capacitance[15] and, consequently, it is also significantly reduced (Table 2). This experiment demonstrates that charge-capacity of the cell is limited by the capacitor-type electrode in hybrid devices obtained by combining a capacitative electrode and one of battery kind. Hence, it is noteworthy the key importance of the existent of an enough charge storage capacity in the limiting electrode that allows to compensate the charges from the redox reaction in order to achieve the maximum performance in this type of hybrid devices.

4.- CONCLUSIONS

The employ of redox active electrolytes is a powerful method to enhance the cell capacitance of carbon-based capacitors. By incorporating MB redox system, an increase of four and a half times the original capacitance value provided by MWCNTs in sulfuric acid was achieved (from 5 to 23 F g-1, expressed as cell capacitance) with no significant increase in the ESR. Moreover, the modified system exhibited an excellent performance at increasing current loads, with a decrease in capacitance of only 10% within the current density range studied. The modified device also fulfills the requirement of long durability necessary for an energy storage system, since after 6000 galvanostatic charge-discharge cycles a reduction of only 12 % in capacitance was observed.

The study of energy storage mechanisms involved in the MB-modified device has revealed that the redox reaction takes place in both electrodes simultaneously in the voltage range of 0-0.104 V, and that this is the main cause of cell capacitance enhancement. Beyond this voltage range, the faradaic contribution from the MB redox reaction decreases because, although the cathode continues to behave as a battery, the anode behaves as a capacitative electrode with a rather reduced charge-capacity due to the small surface area characteristic of MWCNTs. By means of a modified assembly composed of a Nafion membrane and MB and sulfuric acid solutions located in the cathode and anode compartments, respectively, it was demonstrated the limiting role of the capacitative electrode in the cell charge-capacity of hybrid devices obtained by the combination of a capacitor-type electrode and one of a faradaic kind.

ACKNOWLEDGMENT. The authors acknowledge the financial support of the MICINN (Project MAT2010-20601-C02-01). Silvia Roldán thanks MICINN for a FPI predoctoral research grant.

REFERENCES

(1) Burke, A. *J. Power Sources* **2000**, *91*, 37-50.

(2) Kötz, R; Carlen, M. *Electrochim. Acta* **2000**, *45*, 2483.

(3) Simon, P.; Gogotsi, Y. *Nat. Mat.* **2008**, *7*, 845-854.

(4) Frackowiak, E.; Delpeux, S.; Jurewicz, K.; Szostak, K.; Cazorla-Amoros, D.; Béguin, F. *Chemical Physics Letters* **2002,** *361*, 35-41.

(5) Frackowiak, E.; Béguin, F. *Carbon* **2001**, *39*, 937-950.

(6) Jurewicz, K.; Babel, K.; Pitrzak, R.; Delpeux, S.; Wachowska, H. *Carbon* **2006**, *44*, 2368-2375.

(7) Xiao, Q; Zhou, X. *Electrochim. Acta* **2003**, *48*, 575-580.

(8) Jurewicz, K.; Depleux, S.; Bertagna, V.; Béguin, F.; Frackowiak, E. *Chemical Physics Letters* **2002**, *347*, 36-40.

(9) Frackowiak, E.; Metenier, K.; Bertagna, V.; Béguin, F. *Applied Physics Letters* **2000**, *77*, 2421.

(10) Ruz, V.; Santamaría, R.; Granda, M.; Blanco, C. *Electrochimica Acta* **2009**, *54*, 4481.

(11) Frackowiak, E. *Physical Chemistry Chemical Physics* **2007**, *9*, 1774.

(12) Snook, G.A.; Kao,P.; Best, A.S. *Journal of Power Sources* **2011**, *196*, 1.

(13) Roldán, S.; González, Z.; Blanco, C.; Granda, M.; Menéndez, R.; Santamaría, R. *Electrochim. Acta* **2011**, *56,* 3401-3405.

(14) Roldán, S.; Blanco, C.; Granda, M.; Menéndez, R.; Santamaría, R. *Angew. Chem. Int. Ed.* **2011**, *50*, 1699-1701.

(15) Roldán, S.; Granda, M.; Menéndez, R.; Santamaría; R. Blanco, C. *J. Phys. Chem. C* **2011**, *115*, 17606-17611.

(16) Battlebury, D. R. *J. Power Sources* **1999**, *80*, 7-11.

(17) McCreery, R. L. *Chem. Rev.* 108, **2008**, 2646-2687.

(18) Conway, B. E. *Electrochemical Supercapacitors*; Kluwer Academic/Plenum Publishes: New York, 1999, 612.

(19) Pell, W. G.; Conway, B. E. *J. Power Sources* **2004**, *136*, 334-345.

(20) Bodoardo, S.; Borello, L.; Fiorilli, S.; Garrone, E. ; Onida, B. ; Otero Areán, C. ; Penazzi, N.; Turnes Palomino, G. *Micropor. Mesopor. Mater.* **2005**, *79*, 275-281.

(21) Khoo, S. B.; Chen, F. *Anal. Chem.* **2002**, *74*, 5734-5741.

(22) Leventis, N.; Chen, M. *Chem. Mat.* **1997**, *9*, 2621-2631.

(23) Lewis, G. N.; Bigeleisen, J. *J. Am. Chem. Soc* **1943**, *65 (6)*, 1144-1150.

(24) Zaitseva, G.; Gushisem, Y.; Ribeiro, E. S.; Rosatto, S. S. *Electrochim. Acta* **2002**, *47*, 1469-1474.

(25) Kubota, L. T.; Gushikem, Y.; Pérez, J.; Tanaka, A. A. *Langmuir* **1995**, *11*, 1009-1013.

(26) Pumera, M. *Langmuir* **2007**, *23*, 6453-6458.

(27) Lawrence, N. S.; Deo, R. P.; Wang, J. *J. Electroanalysis*, **2005**, *17*, 65-72.

(28) Sljukic, B.; Banks, C. E.; Compton, R. G. *Nano Lett.* **2006**, *6*, 1556-1558.

(29) Zhang, J.; Comotti, M.; Schüth, F.; Schögl, R.; Su, D. S. *Chem. Comm.* **2007**, 1916-1918.

(30) Matter, P. H.; Wang, E.; Millet, J. M.; Ozkan, U. S. *J. Phys. Chem. C.* **2007**, *111*, 1444-1450.

(31) Lyon, J. L.; Stevenson, K. J. *Langmuir* **2007**, *23*, 11311-11318.

(32) Bard, A. J.; Faulkner, L. R. *Electrochemical Methods: Fundamentals and Applications*; John Wiley and Sons: New York, 2001.

(33) Conway, B. E.; Birss, V.; Wojtowicz, J. *J. Power Sources* **1997**, *66*, 1-14.

FIGURE CAPTIONS

Figure 1. Comparison of the electrochemical responses of the two-electrode cells in the MB solution and in the supporting electrolyte at 1 V: a) variation of the cell specific capacitance values with the

current load (from 0.88 to 88.4 mA cm^{-2}), b) galvanostatic cycles at 0.88 mA cm^{-2} and c) cyclic voltammograms at 2 mV s^{-1}.

Figure 2. a) Cyclic voltammograms obtained in a three-electrode cell with the MB solution and with the supporting electrolyte at a scan rate of 2 mV s^{-1}. b) Anodic and cathodic peak current dependence on the square root of the scan rate.

Figure 3. Galvanostatic cycle at 1 V (left Y-axis) and the working potentials for the positive and negative electrodes (right Y-axis) obtained in: a) H_2SO_4 and b) MB solutions, using a T-Type Swagelok cell. c) Voltage profiles obtained in a T-type Swagelok cell modified by employing a Nafion membrane as separator and the H_2SO_4 and MB solutions in the anode and cathode, respectively. Current density 8.8 mA/cm^2.

SCHEME TITLES

Scheme 1. Redox process of Methylene blue in acid media.

Scheme 2. Representation of: a) the device resulting of the incorporation of MB in the original EDLC, in which the MB solution is used in both electrodes, and b) cell with a Nafion membrane as separator and solutions of MB and sulphuric acid located separately in the cathode and anode compartments, respectively. In system a) all ions can pass through the separator, while in system b) only protons are able to pass through the Nafion membrane.

TABLES

Table 1. Cell and electrode capacitances of the three systems analyzed: the original EDLC, the system resulting from the incorporation of MB in the original capacitor (MB-modified device), and the system modified by a Nafion membrane (Nafion-modified device).

	Cell		*Anode*		*Cathode*	
	C_{cell} (F)	$C_{esp,\ cell}$ (F g^{-1})	C_{elec+} (F)	$C_{esp,\ elec+}$ (F g^{-1})	C_{elec+} (F)	$C_{esp,\ elec+}$ (F g^{-1})
EDLC	0.3	5	0.6	21	0.6	20
MB-modified device	1.2	23	1.7	71	3.6	131
Nafion-modified device	0.8	14	0.8	31	7.6	279

Table 2. Voltage ranges and operating potential intervals of the electrodes divided in function of the different types of behaviour shown by the MB-modified device.

	Region I	*Region II*	*Region III*
	Battery-type behaviour	Hybrid behaviour	Capacitor-type behaviour
Cell (V)	0 to 0.104	0.104 to 0.709	0.709 to 0.994
Anode (V vs. Hg/Hg_2SO_4)	-0.2 to -0.142	-0.142 to 0.432	0.432 to 0.482
Cathode (V vs. Hg/Hg_2SO_4)	-0.2 to -0.259	-0.259 to -0.350	-0.350 to -0.529

SYNOPSIS TOC

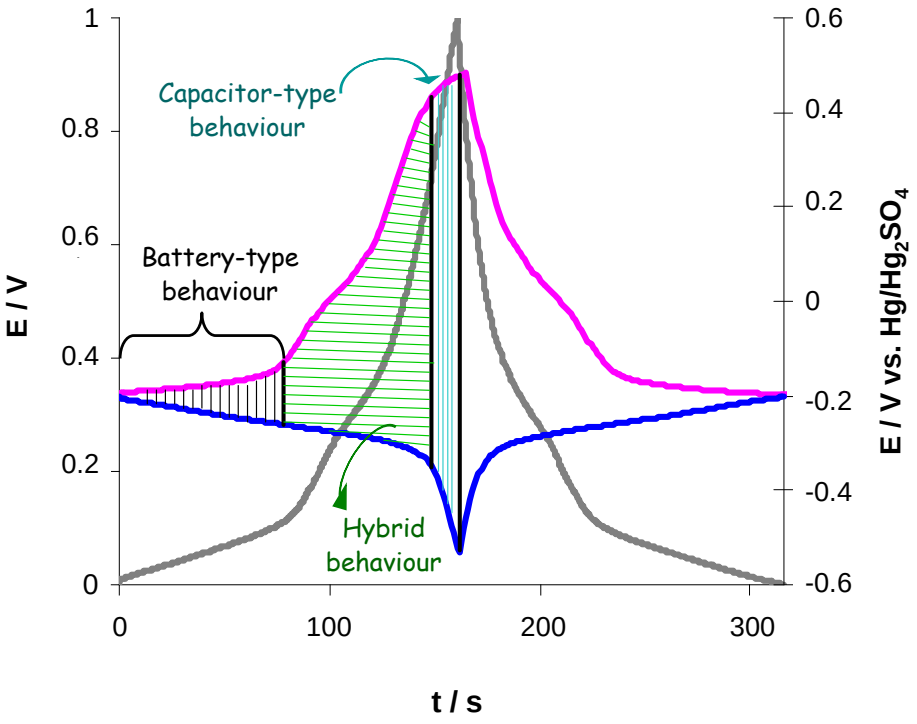
Capacitor-type
behaviour
Battery-type
behaviour
Hybrid
behaviour
E / V
E / V vs. Hg/Hg2SO4
t / s
1
0.8
0.6
0.4
0.2
0
0.6
0.4
0.2
0
-0.2
-0.4
-0.6
0
100
200
300

Scheme 1. Redox process of Methylene blue in acid media.

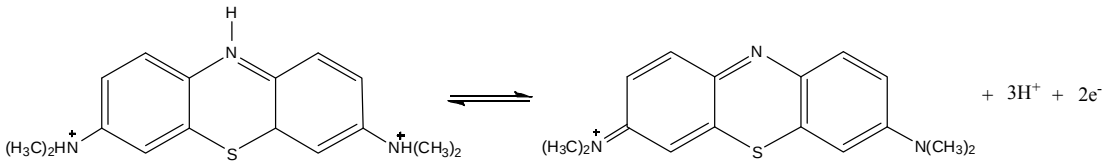

Reduced Methylene Blue Oxidized Methylene Blue

Scheme 2. Representation of: a) the device resulting of the incorporation of MB in the original EDLC, in which the MB solution is used in both electrodes, and b) cell with a Nafion membrane as separator and with the MB solution and the supporting electrolyte located separately in the cathode and anode compartments, respectively. In system a) all ions can cross over the separator, while in system b) only protons are able to pass through the Nafion membrane.

a)

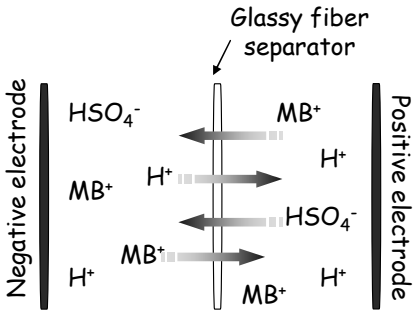

b)

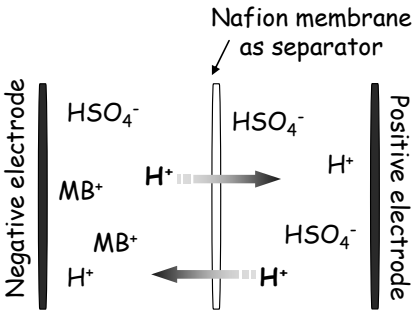

Figure 1. Comparison of the electrochemical response of the two-electrode cells in the MB solution and in the supporting electrolyte at 1 V: a) variation of the cell specific capacitance values with the current load (from 0.88 to 88.4 mA cm^{-2}), b) galvanostatic cycles at 0.88 mA cm^{-2} and c) cyclic voltammograms at 2 mV s^{-1}.

a)

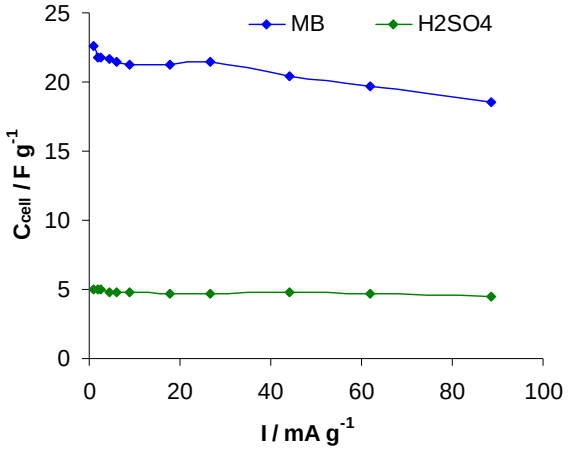

b)

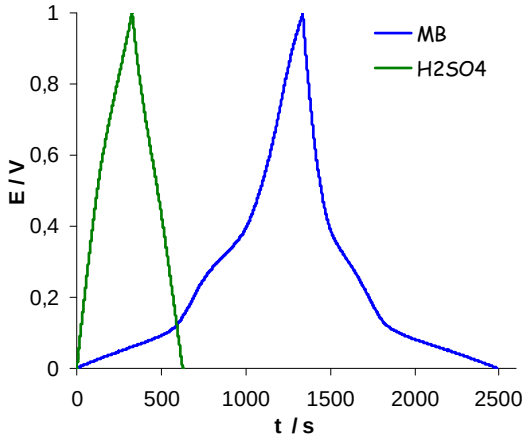

c)

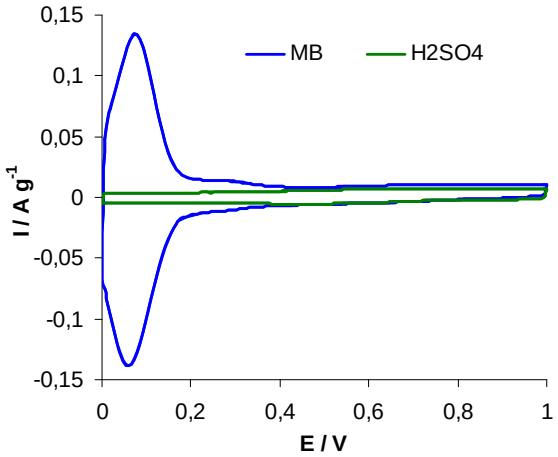

Figure 2. a) Cyclic voltammograms obtained in a three-electrode cell in the MB solution and in the supporting electrolyte at scan rate of 2 mV s^{-1}. b) Anodic and cathodic peak current dependence on the square root of the scan rate.

a)

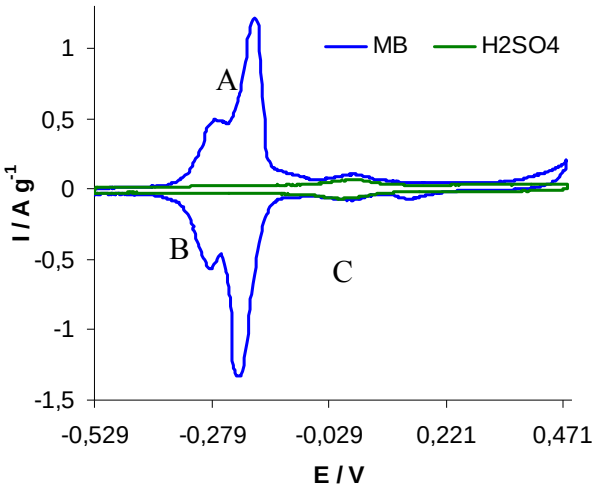

b)

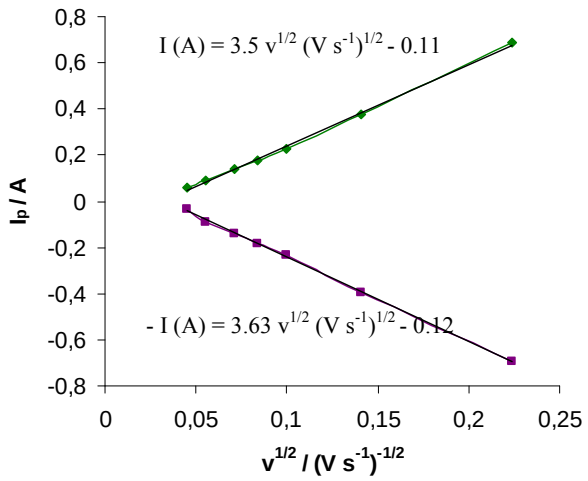

Figure 3. Galvanostatic cycle at 1 V (left Y-axis) and the working potentials for the positive and negative electrodes (right Y-axis) obtained in: a) H_2SO_4 and b) MB solution, using a T-Type Swagelok cell. c) Voltage profiles obtained in a T-type Swagelok cell modified employing a Nafion membrane as separator and the H_2SO_4 and MB solutions in the anode and cathode, respectively. Current density 8.8 mA/cm^2.

a)

b)

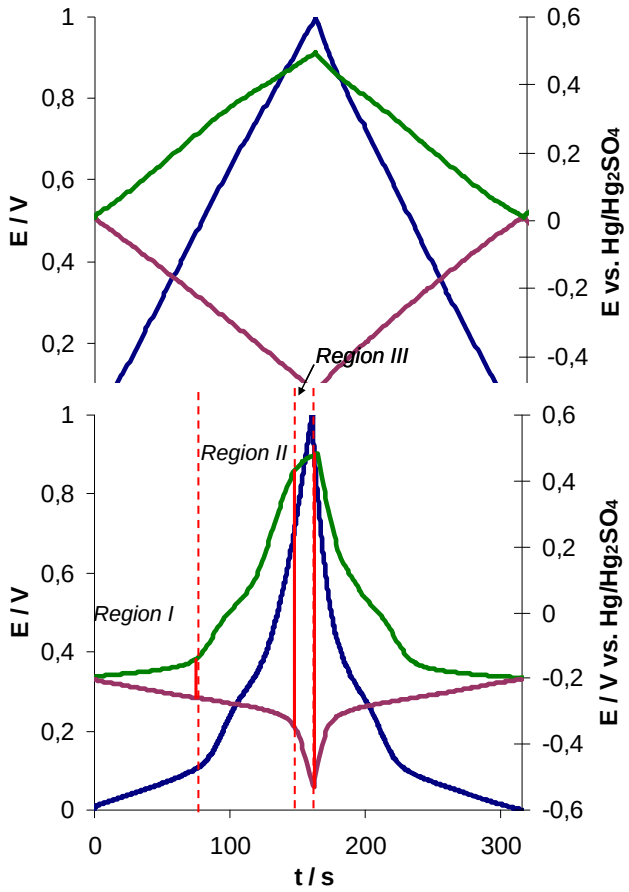

c)